Cancer Management and Research

Dovepress
open access to scientific and medical research

Open Access Full Text Article

ORIGINAL RESEARCH

TINAGL1 promotes hepatocellular carcinogenesis through the activation of TGF-β signaling-medicated VEGF expression

This article was published in the following Dove Medical Press journal:
Cancer Management and Research

Cancer Management and Research downloaded from https://www.dovepress.com/
For personal use only.

Lu Sun[1,2]
Zihui Dong[3]
Hongli Gu[2]
Zhixian Guo[2]
Zujiang Yu[2]

[1]Department of Gastroenterology, The First Affiliated Hospital of Zhengzhou University, Zhengzhou, Henan, China; [2]Department of Infectious Disease, The First Affiliated Hospital of Zhengzhou University, Zhengzhou, Henan, China; [3]Department of Precision Medicine Center, The First Affiliated Hospital of Zhengzhou University, Zhengzhou, Henan, China

Background and purpose: Tubulointerstitial nephritis antigen-like 1 (TINAGL1) is an extracellular matrix protein that plays an important role in cell adhesion and therefore modulates cell proliferation, migration, and differentiation. In addition, it is frequently upregulated in highly metastatic tumors. The aim of our study was to determine the role of TINAGL1 in the progression and metastasis of hepatocellular carcinoma (HCC).

Materials and methods: TINAGL1 mRNA levels were analyzed in HCC and adjacent non-tumorous samples by reverse transcription polymerase chain reaction (RT-PCR). Human HCC cell lines were transfected with lentiviral plasmids expressing either si-TINAGL1 or TINAGL1 and subjected to CCK-8, colony forming, transwell migration, Annexin V/propidium iodide, and 5-ethynyl-2′-deoxyuridine uptake assays. Suitably transfected HCC cells were injected into athymic nude mice to establish xenograft tumors that were imaged and measured on a weekly basis. Mediators of the TGF-β signaling pathway were analyzed by Western blot.

Results: TINAGL1 was upregulated in human HCC tissues and associated with poor prognosis. TINAGL1 knockdown suppressed HCC cell growth, proliferation, and migration and induced apoptosis in HCC cells, whereas TINAGL1 overexpression had opposite effects. In addition, inhibition of TINAGL1 retarded xenograft tumor growth in a nude mouse model. Mechanistically, TINAGL1 activated the TGF-β signaling pathway and increased VEGF secretion.

Conclusion: TINAGL1 promotes hepatocellular carcinogenesis and metastasis via the TGF-β/Smad3/VEGF axis and is a potential new biomarker of HCC.

Keywords: TINAGL1, LCN7, hepatocellular carcinoma, TGF-β, VEGF

Introduction

Hepatocellular carcinoma (HCC), the most common malignant cancer among humans, is the third major leading cause of deaths worldwide.[1,2] Most patients are diagnosed at the advanced stage of the disease and therefore have poor prognosis.[3,4] In addition to traditional therapies like trans-arterial chemoembolization, surgical resection, or organ transplantation, chemotherapeutic agents like sorafenib are increasingly being used to treat the advance tumors. Although sorafenib enhances survival rate, HCC resistance and recrudesce will appear later on.[5] Patients treated with sorafenib have only 2–3 months survival benefit compared with no therapeutic patients.[6,7] Therefore, it is essential to identify novel biomarkers of HCC in order to improve therapeutic outcomes.

Tubulointerstitial nephritis antigen-like 1 (TINAGL1), formerly known as lipocalin 7 (LCN7), adrenocortical zonation factor-1 (AZ1), and tubulointerstitial nephritis antigen-related protein (TIN-ag-RP), is an extracellular matrix (ECM) protein that promotes

Correspondence: Zujiang Yu
Department of Infectious Disease, The First Affiliated Hospital of Zhengzhou University, No 1 Construction East Road 1, Erqi District, Zhengzhou 450052, Henan, China
Tel +86 183 3712 8258
Email ZujiangY@126.com

submit your manuscript | www.dovepress.com
Dovepress
http://dx.doi.org/10.2147/CMAR.S190390

© 2019 Sun et al. This work is published and licensed by Dove Medical Press Limited. The full terms of this license are available at https://www.dovepress.com/terms.php and incorporate the Creative Commons Attribution – Non Commercial (unported, v3.0) License (http://creativecommons.org/licenses/by-nc/3.0/). By accessing the work you hereby accept the Terms. Non-commercial uses of the work are permitted without any further permission from Dove Medical Press Limited, provided the work is properly attributed. For permission for commercial use of this work, please see paragraphs 4.2 and 5 of our Terms (https://www.dovepress.com/terms.php).

cell adhesion[8] and migration by binding to integrins such as a1b1 (ITGA1B1), a2b1 (ITGA2B1), and a5b1 (ITGA5B1).[9] The integral sequences of TINAGL1 include the N-terminal EGF-like domains, a follistatin motif, and a C-terminal cathepsin B-like domain.[10] Aberrant TINAGL1 expression has been observed in various pathophysiological situations.[11] For example, Mary et al[12] found that TINAGL1 protein was downregulated in the placenta of pre-eclamptic women and female TINAGL1 knockout mice suffered from infertility.[13] TINAGL1 was also upregulated in the cardiac ECM in a porcine model of ischemia/reperfusion injury.[14] In addition, Umeyama et al[15] found that TINAGL1 is a pro-metastatic factor in non-small-cell lung cancer, while another study reported an anti-metastatic role in breast cancer,[16] and it was also demonstrated to be upregulated in some highly metastatic cancers.[17] The role of TINAGL1 in HCC is hitherto unknown.

In the present study, we found that TINAGL1 mRNA and protein levels were significantly higher in the HCC tissues compared to those in the adjacent non-tumor tissues. In addition, ectopic expression of TINAGL1 in HCC cells increased proliferation and migration and inhibited apoptosis. TINAGL1 inhibition significantly retarded the growth of tumor xenografts in nude mice. Further bioinformatics and functional analyses indicated that TINAGL1 mediated its effects in the HCC cells via the TGF-β/Smad3/VEGF axis. Taken together, we present a novel mechanism of hepatocellular carcinogenesis as well as a potential new prognostic biomarker and therapeutic target for HCC.

Materials and methods

Tumor samples

Tumor and matched non-tumor tissues (38 pairs) were collected after surgical resection at the First Affiliated Hospital of Zhengzhou University, and ~2 cm pieces were snap frozen for subsequent analysis. Our study was approved by the Institutional Review Board of Zhengzhou Medical University and conducted in accordance with the 1964 Declaration of Helsinki and its later amendments or comparable ethical standards. All patients provided signed informed consent. In all, 0.5 g minced tissues were digested in ice with RIPA, phenylmethanesulfonyl fluoride (PMSF), and protease inhibitor after washing with cold normal saline and then examined by Western blot. Besides, the other parts of minced tissues were used to prepare DNA for reverse transcription polymerase chain reaction (RT-PCR) by homogenate.

Cell lines and cell culture

The human HCC cell lines Hep3B, Huh7, SMMC-7721, HepG2, MHCC-97H, HCC-LM3, and QGY-7703 and the human immortalized normal liver epithelial cell line L02 were acquired from the Cell Bank of the Shanghai Institutes for Biological Sciences. HCC cell lines were cultured in DMEM (Beijing Solarbio Science & Technology Co., Ltd, Beijing, China) supplemented with 10% FBS (Thermo Fisher Scientific, Waltham, MA, USA). L02 cells were cultured in RPMI-1640 medium (Solarbio) with 10% FBS. All cells were fostered in a humidified incubator under 5% CO_2 at 37°C.

Lentiviral preparation and infection

Lentivirus plasmids were constructed by GenePharma (Shanghai, China). SMCC-7721 cells were transduced with LV3-TINAGL1or LV3-NC according to the manufacturer's instructions. Similarly, the HCC-LM3 cells were transduced with LV5-TINAGL1/LV5-NC viral particles. Cells were harvested 72 hours post transduction and validated by fluorescence microscopy (Olympus Corporation, Tokyo, Japan), RT-PCR, and Western blot.

Real-time PCR

Total RNA was extracted from cells and tissue samples using TRIzol reagent (Takara Biomedical Technology Co., Ltd., Beijing, China) according to the manufacturer's protocol, and 1 μg RNA from each sample was reverse transcribed using PrimeScript™ RT Reagent Kit (Perfect Real Time; Takara). Real-time PCR was performed using the SYBR Premix Ex Taq™ (Takara) on the StepOnePlus™ Real-Time PCR cycler (Thermo Fisher Scientific) with the following reaction conditions: 95°C for 30 seconds, followed by 40 cycles of 95°C for 10 seconds, 60°C for 34 seconds, 95°C for 15 seconds, 60°C for 1 minute, and 95°C for 15 minutes. Relative change in gene expression was calculated with the $\Delta\Delta C_t$ method using GAPDH as the internal control. Every sample was analyzed in triplicates.

Western blot

Total protein was extracted from cells and tissues using RIPA buffer supplemented with PMSF. Equal amounts of proteins (30 μg) per sample were separated by 10% SDS-PAGE and transferred to polyvinylidene difluoride membranes. After blocking in 5% skim milk for 1 hour, the membranes were washed thrice with tris-buffered saline (TBS) and incubated overnight at 4°C with the following primary antibodies (all from Proteintech, Wuhan, China): TINAGL1 (1:1,000, 12077-1-AP), Smad3 (1:1,000, 25494-1-AP), VEGF (1:1,000, 19003-1-AP), and GAPDH (1:1,000, 10494-1-AP). After washing thrice with TBS, the blots were incubated with the fluorescence-conjugated goat anti-mouse and goat anti-rabbit secondary antibodies (1:5,000; Sigma-Aldrich

Co., St Louis, MO, USA) at room temperature for 1 hour. The positive bands were observed by infrared laser scanning imaging system (Odyssey CLx; General Electric Company, Boston, MA, USA).

Cell proliferation assays

The infected cells were seeded into 96-well plates at the density of 2×10^3/well and cultured for 5 days. Every 24 hours, 10 μL CCK-8 reagent (TransGen Biotech Co. Ltd., Beijing, China) was added to each well, and the absorbance at 450 nm was measured using a Microplate System after 2 hours incubation. Cells in the logarithmic phase of growth were seeded into six-well plates at the density of 1×10^3 cells/well and cultured for 14 days. After fixing the colonies with paraformaldehyde for 30 minutes, they were stained with 1% crystal violet (Sigma-Aldrich Co.). Aggregates of ≥50 cells (0.3–1.0 mm) were considered as colonies and counted.

Transwell migration assay

Transfected cells were seeded into the upper chamber of transwell inserts (Corning Incorporated, Corning, NY, USA) at the density of 1×10^5/well in 200 μL serum-free media, and the lower chamber was filled with 500 μL media containing 10% serum. After 24 hours incubation, the cells that migrated to the bottom surface of the filters were fixed with 4% formaldehyde and stained with crystal violet. Cells were counted in eight randomly selected fields from each well using a fluorescence microscope. The cell invasion assay was performed using Matrigel-coated transwell inserts using the same method as described.

5-Ethynyl-2′-deoxyuridine (EdU) uptake assay

DNA synthesis was evaluated by the uptake of EdU, a thymidine analog that is a substitute for thymine (T) in the replicating cells. Transduced cells were seeded into 24-well plates at the density of 5×10^4 cells/well and analyzed using the Cell-Light™ EdU Apollo® 488 In Vitro Imaging Kit (Guangzhou RiboBio Co. Ltd., Guangzhou, China) according to the manufacturer's instructions. The cells were then observed and imaged using a fluorescence microscope.

Annexin V/propidium iodide (PI) staining

Infected cells were harvested using trypsin solution without EDTA (Solarbio) and stained with PI for 15 minutes in the dark. The stained cells were acquired by FACScan flow cytometer (BD Biosciences, San Jose, CA, USA) to distinguish between the early apoptotic (Annexin V+/PI–), middle and late apoptotic (Annexin V+/PI+), and dead (Annexin V–/PI+) cells.

Xenograft establishment in nude mice

Animal experiments were performed in compliance with the guidance of the ethics committee of Institute of Medicine, University of Zhengzhou, Henan Province and approved by the committee. Five-week-old male BALB/c nude mice (n=12) were purchased from the Vital River Laboratory Animal Technology Co. Ltd. (Beijing, China) and randomly divided into two groups, and 2×10^6 SMCC-7721 cells infected with si-TINAGL1 or LV3-NC were injected subcutaneously into each mouse (in 200 μL). The tumor volume and weight were monitored twice a week, and the tumors were imaged every week using the IVIS@Lumina III system (Caliper Life Sciences, Hopkinton, MA, USA). The mice were euthanized with CO_2 30 days post inoculation, and the tumor masses were resected.

Statistical analyses

All statistical analyses were performed using SPSS 17.0 (SPSS Inc., Chicago, IL, USA) software. Data were presented as the mean ± SD values, and statistical analysis was performed using paired *t*-test or Student's *t*-test. *P*-value <0.05 was considered as statistically significant.

Results

TINAGL1 is upregulated in human HCC tissues and cell lines

As shown in Figure 1A–C, TINAGL1 mRNA levels were significantly higher in the HCC tissues compared with the paired adjacent non-cancerous tissues. In addition, the TINAGL1 protein and mRNA levels were also higher in four randomly selected tumors compared to their corresponding normal tissues (Figure 1C), which is consistent with the expression of TINAGL1 in the seven HCC cell lines compared to the normal liver epithelial cells (Figure 1D). The SMCC-7721 and HCC-LM3 cell lines were selected for the subsequent experiments since the expression of TINAGL1 was respectively the highest and lowest in these cells.

TINAGL1 is a biomarker of HCC and its overexpression is associated with poor prognosis

The 38 HCC patients were divided into the TINAGL1 high- and low-expressing groups based on the median TINAGL1 mRNA expression levels. The association between TINAGL1 expression and the clinicopathological characteristics of the patients is summarized in Table 1. The TINAGL1^{high} patients

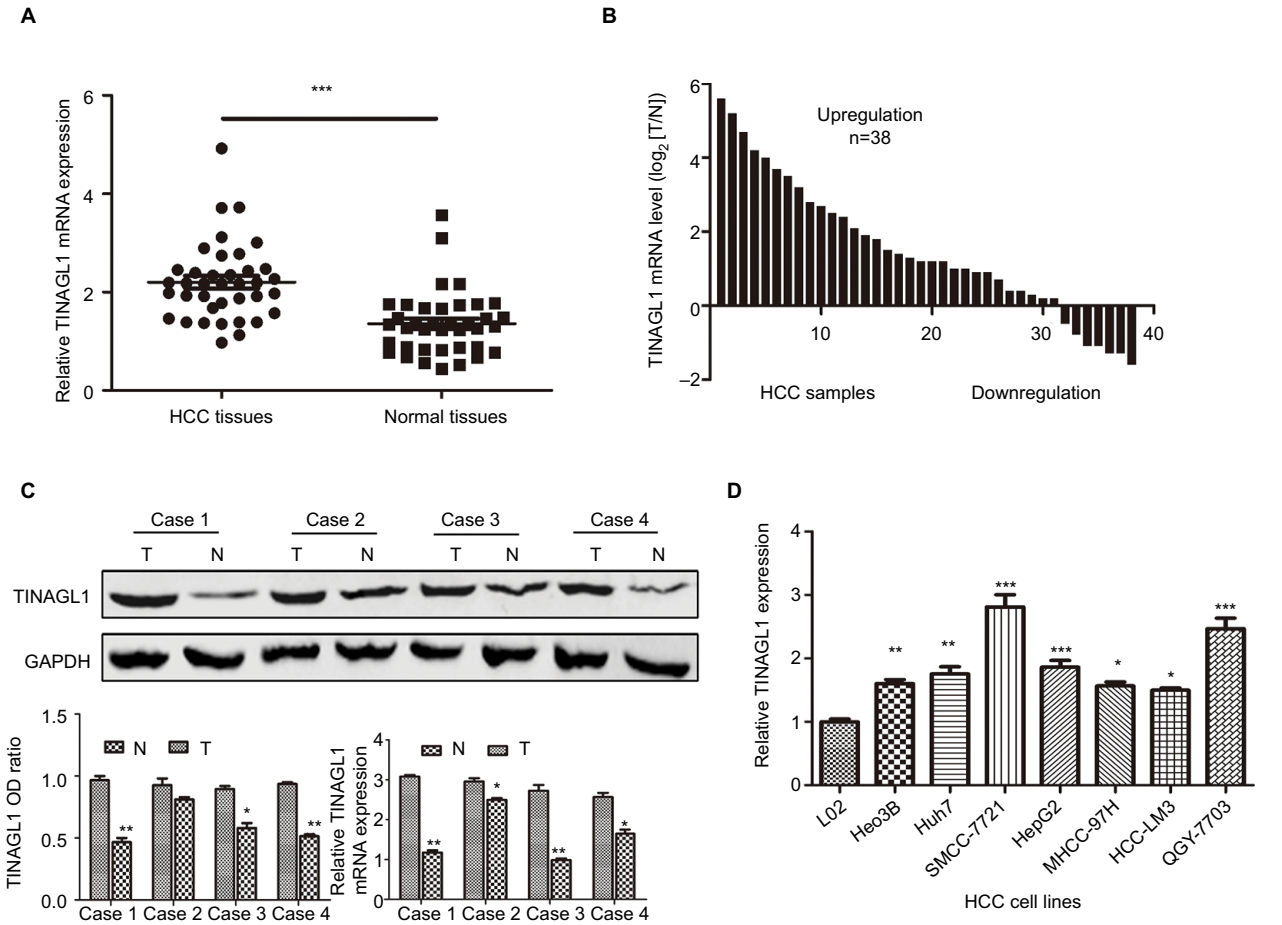

Figure 1 TINAGL1 is upregulated in HCC samples and HCC cell lines.

Notes: (**A** and **B**) TINAGL1 mRNA levels in the HCC and non-cancerous tissues showing upregulation in 31/38 (81.6%) of the HCC tissues. (**C**) Western blots showing TINAGL1 protein levels in four randomly selected tissue pairs, normalized to GAPDH. (**D**) TINAGL1 mRNA levels in seven HCC cell lines were higher than those in L02 cells. **P*<0.05; ***P*<0.01; ****P*<0.001.

Abbreviation: HCC, hepatocellular carcinoma.

had shorter overall survival (OS) and progression-free survival (PFS) compared to the TINAGL1^{low} patients (Figure 2A and B), and multivariate analysis demonstrated that TINAGL1 was an independent risk factor for OS (Figure 2C). Taken together, TINAGL1 is predictive of worse prognosis and is a potential biomarker of HCC.

TINAGL1 promotes HCC cell proliferation and survival

The aberrant expression of TINAGL1 in HCC cells indicates its involvement in HCC biology. To confirm our hypothesis, we knocked down TINAGL1 in SCC-7721 cells and overexpressed it in the HCC-LM3 cells. The TINAGL1 mRNA and protein levels in both cell lines were validated by RT-PCR and Western blot, respectively (Figure 3A and B), and si-TINAGL1-1 was selected for further experiments due its maximum inhibitory effect. As shown in Figure 3C and D, TINAGL1 knockdown inhibited the proliferation of SMCC-7721 cells and restrained colony formation, whereas the TINAGL1-overexpressing HCC-LM3 cells grew faster and produced numerous colonies compared to the control cells. In addition, si-TINAGL1 inhibited HCC cell migration in vitro, while TINAGL1 had the opposite effects (Figure 3E). Consistent with this, TINAGL1 silencing and overexpression respectively decreased and increased DNA synthesis as measured in terms of EdU uptake (Figure 3F). Finally, TINAGL1 also decreased apoptosis in the HCC cells, while si-TINAGL1 induced cell apoptosis (Figure 3G). Taken together, TINAGL1 promotes the proliferation, survival, and metastasis of HCC cells in vitro.

Effect of TINAGL1 on the growth of tumor in nude mice

To evaluate the effect of TINAGL1 on tumor growth in vivo, SMCC-7721 cells transfected with si-TINAGL1 were injected

Table 1 The association between TINAGL1 and clinical characteristics in HCC tissues

Clinicopathological features	Factors	TINAGL1^{low} expression	TINAGL1^{high} expression	*P*-value
Age (years)	≤50 >50	15 9	11 3	0.472
Gender	Male Female	13 5	12 8	0.506
TNM stage	I, II III, IV	12 5	6 15	**0.021**
Tumor size (cm)	≤5 >5	12 4	8 14	**0.025**
Metastasis	Yes No	5 12	14 7	**0.049**
AFP	≤30 >30	7 8	9 14	0.743

Note: The *P*-values with significance are marked in bold.
Abbreviations: AFP, alpha fetoprotein; HCC, hepatocellular carcinoma.

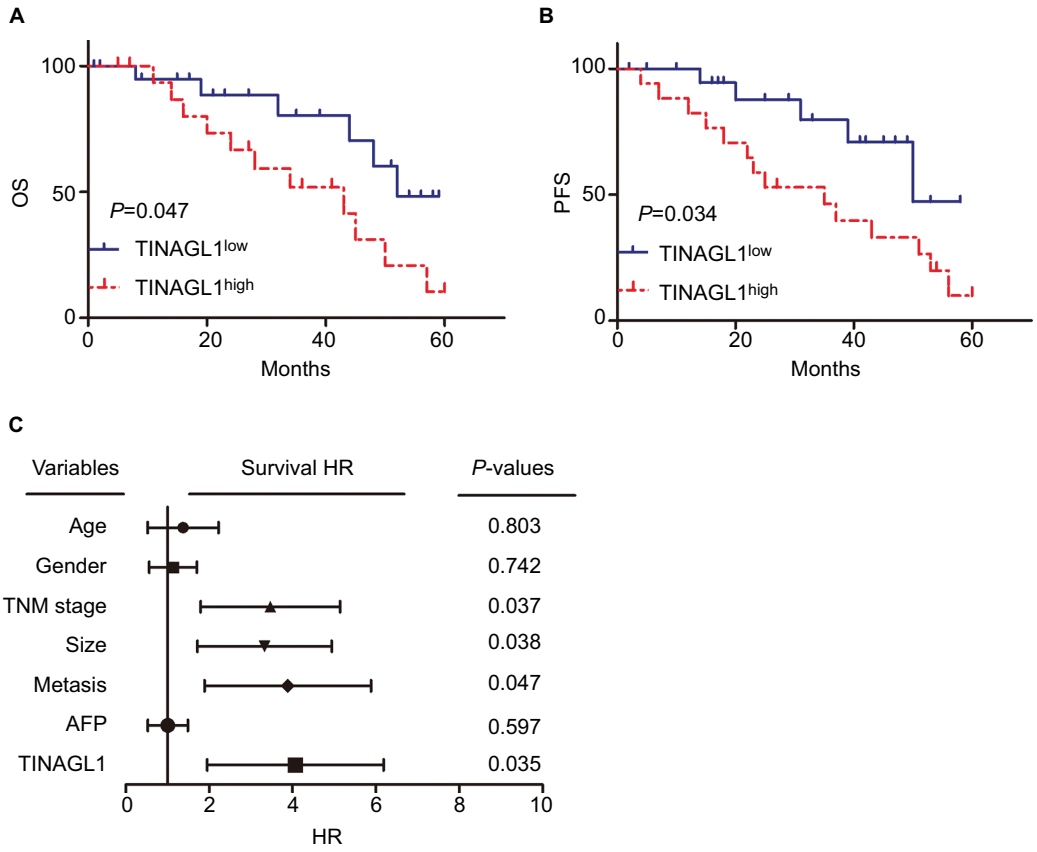

Figure 2 TINAGL1 is a biomarker of HCC and associated with poor prognosis.
Notes: Kaplan–Meier curves showing OS (**A**) and PFS (**B**) of TINGL1^{high} and TINAGl1^{low} HCC patients. (**C**) Forest plot showing that TINAGL1 overexpression is an independent prognostic factor for OS.
Abbreviations: HCC, hepatocellular carcinoma; OS, overall survival; PFS, progression-free survival.

subcutaneously in athymic nude mice (n=12). As shown in Figure 4A, the tumor masses arising from the TINAGL1-knockdown cells were significantly smaller compared to those originating from LV3-NC cells. In addition, the transfected cells were tagged with the generated green fluorescent protein (GFP), which enabled in vivo imaging and monitoring of the tumors. The GFP+ tumor area and intensity were both lower in the si-TINAGL1 group (Figure 4B). Consistent with this, TINAGL1 knockdown significantly decreased tumor volume and weight compared to the control tumors (Figure 4C and D).

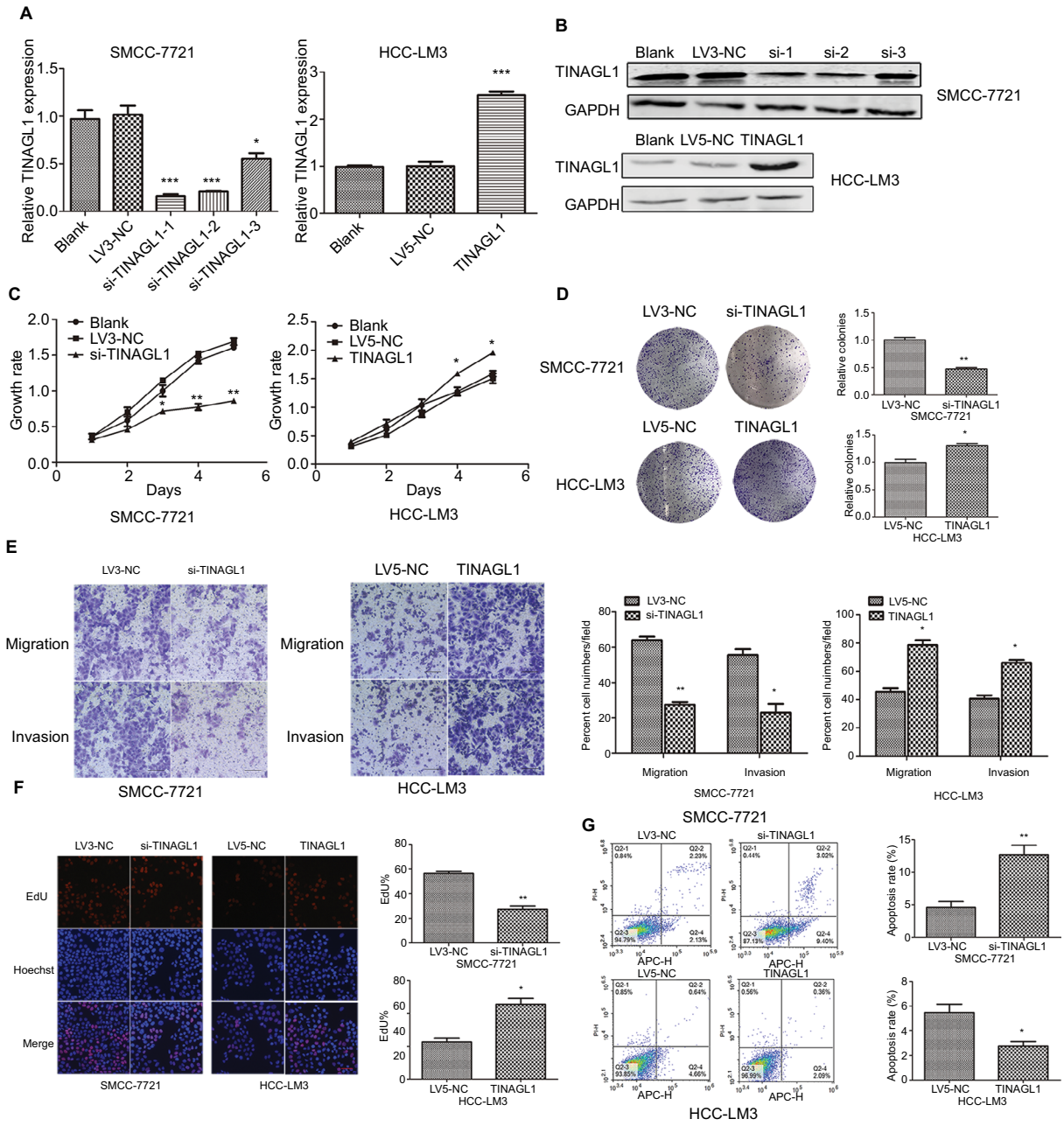

Figure 3 TINAGL1 promotes HCC cell survival.

Notes: (**A** and **B**) RT-PCR and Western blot showing TINAGL1 mRNA and protein levels in HCC cells transfected with si-TINAGL1 or TINAGL1. (**C** and **D**) The proliferation and colony formation rates of the transfected cells. (**E**) Migration and invasion of the transfected cells as demonstrated by the transwell assay; bar =50 μm. (**F**) EdU uptake (red) in cells counterstained with Hoechst (blue); bar =200 μm. (**G**) Annexin V/PI stained cells showing apoptosis rates. *P<0.05; **P<0.01; ***P<0.001.

Abbreviations: EdU, 5-ethynyl-2′-deoxyuridine; HCC, hepatocellular carcinoma; PI, propidium iodide; RT-PCR, reverse transcription polymerase chain reaction.

As expected, the TINAGL1 protein levels in the tumor tissues were significantly lower in the si-TINAGL1 group (Figure 4E).

TINAGL1 exerts its pro-tumorigenic effects by activating the TGF-β and VEGF signaling pathways

To further investigate the mechanisms underlying the pro-survival role of TINAGL1 in HCC, gene set enrichment analysis (GSEA) was performed to predict the related signaling pathways. The gene expression profiles of 374 patients were obtained from The Cancer Genome Atlas database, and the cohort was classified into the TINAGL1^{high} and TINAGL1^{low} groups. Out of the 186 curated KEGG gene sets, the TGF-β and VEGF signaling pathways were significantly enriched in the TINAGL1^{high} group (Figure 5A), indicating the potential role of both pathways in mediating the effects of TINAGL1.

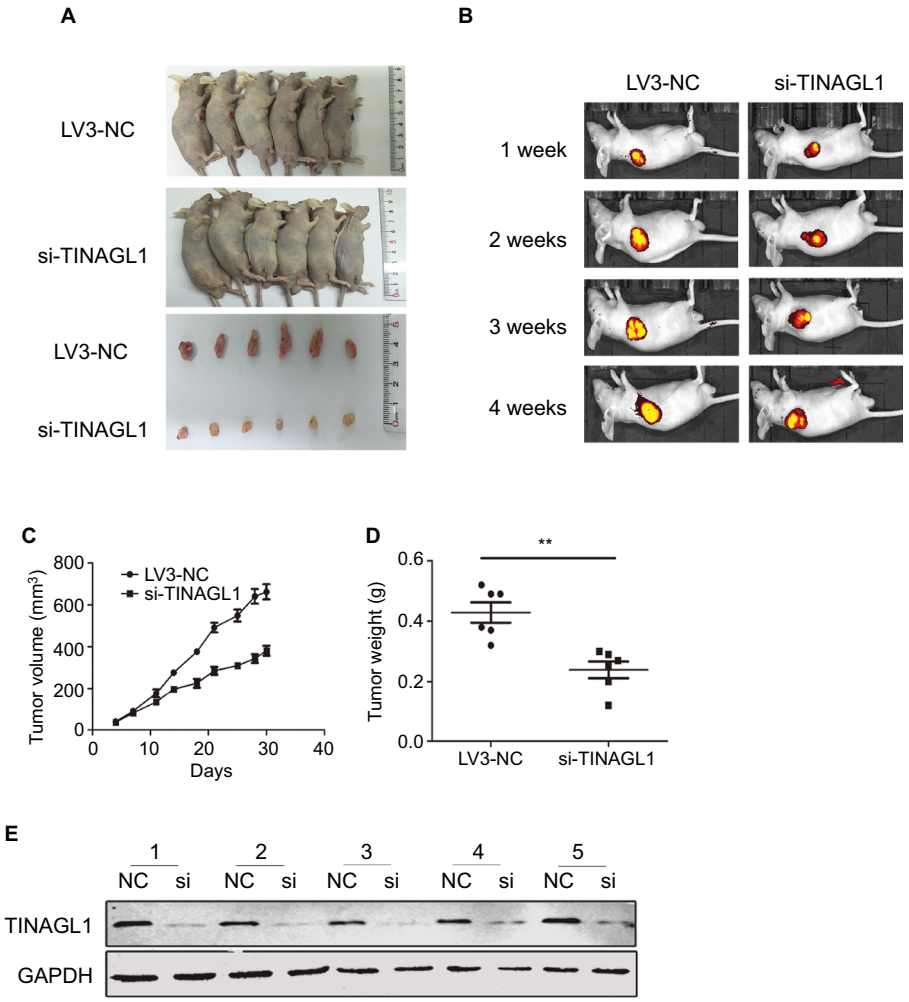

Figure 4 Effect of TINAGL1 on the growth of tumor in nude mice.
Notes: (**A**) Tumor masses in the different mouse groups. (**B**) In vivo fluorescence imaging of tumors 1, 2, 3, and 4 weeks after inoculation. (**C** and **D**) Tumor volume and weight in different mouse groups. (**E**) Western blots showing TINAGL1 expression in the tumor tissues of different groups. $^{**}P<0.01$.

Since reports indicated that TGF-β could increase VEGF secretion in cancer cells,[20,21] we hypothesized that TGF-β and VEGF signaling pathways participated in the accelerating effect of TINAGL1 in HCC cells. In our study, HCC cells stimulated with 5 ng/mL TGF-β (R&D Systems Inc., Minneapolis, MN, USA) showed Smad3 activation and VEGF secretion. In addition, TINAGL1 upregulated both Smad3 and VEGF, while inhibition of Smad3 by SB431542 (Santa Cruz Biotechnology Inc., Dallas, TX, USA) suppressed VEGF secretion (Figure 5B). To determine the functional relevance of TGF-β/Smad3 in TINAGL1-overexpressing HCC-LM3 cells, 10 μM SB431542 or 1 μM SU5416 (VEGF inhibitor; WuXi AppTec, Shanghai, China) was added for further study. As shown in Figure 5C–E, blockade of TGF-β signaling abrogated the enhanced growth, proliferation, migration, and invasion induced by TINAGL1 in HCC-LM3 cells down to baseline levels. Taken together, TINAGL1 promotes hepatocellular carcinogenesis in vitro via TGF-β/Smad3/VEGF signaling.

Discussion

HCC is a malignant tumor with a high recurrence rate; the key point is complexity of cancer stem cell-dependent field cancerization.[22] Despite improvements in cancer surveillance and therapy, the prognosis for HCC remains unsatisfactory due to the high incidence of recurrence and metastasis.[23,24] It is essential to elucidate the mechanisms underlying HCC progression and identify novel biomarkers in order to improve prognosis and therapeutic outcome.[25]

TINAGL1 is expressed in vascular tissues[9,26] and has been previously shown to be aberrantly expressed in tumors.[15,16] As shown in the present study, TINAGL1 was significantly

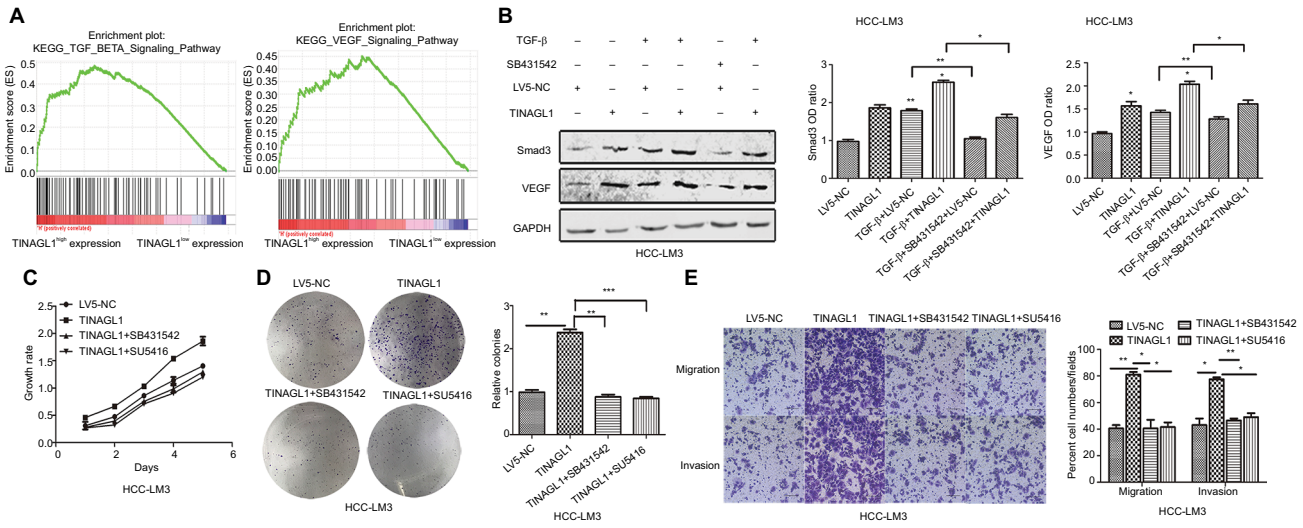

Figure 5 TINAGL1 promotes HCC cell proliferation and migration via the TGF-β/Smad3/VEGF axis.
Notes: (**A**) GSEA results showing significant enrichment of the TGF-β and VEGF signaling pathways in the TINAGL1^{high} patients from the TCGA liver cancer cohort. (**B**) Western blots showing Smad3 and VEGF levels in HCC cells in response to TGF-β, TINAGL1, and SB431542 (Smad3 inhibitor). (**C**–**E**) Functional assays on TINAGL1-overexpressing HCC-LM3 cells treated with SB431532 and SU5416 (VEGF inhibitor); bar =50 μm. *P<0.05; **P<0.01; ***P<0.001.
Abbreviations: HCC, hepatocellular carcinoma; GSEA, gene set enrichment analysis; TCGA, The Cancer Genome Atlas.

upregulated in HCC tissues compared to the adjacent normal samples. In addition, we found a strong positive correlation between TINAGL1 levels and the tumor grade and OS of HCC patients. TINAGL1 silencing in the SMCC-7712 cells inhibited proliferation, migration, and invasion and induced apoptosis, while the overexpression of TINAGL1 in HCC-LM3 cells had the opposite effects. Furthermore, TINAGL1 inhibition also delayed xenograft tumor formation and impeded tumor growth in nude mice. Taken together, TINAGL1 acts as an oncogene in HCC and is a potential therapeutic target for HCC.

GSEA showed a significant enrichment of the TGF-β and VEGF signaling pathways in the TINAGL1^{high} dataset, indicating that both pathways mediate TINAGL1 function in the HCC cells. The TGF-β is a well-known oncogene that regulates the cell differentiation, proliferation, and apoptosis[27,28] and acts as a tumor promoter in the disease state.[29,30] TGF-β1 could mediate the activation of certain downstream targets of the PI3K (Jnk and Erk) signaling pathway.[31] However, the most prominent intracellular mediators of TGF-β signaling are the Smad proteins (Smad2 and Smad3), which form trimeric complexes, translocate to the nucleus, and regulate the transcription of several genes.[32] Both Smad3 and VEGF were upregulated in the HCC cells upon TGF-β stimulation, which was consistent with previous studies.[18,19] In addition,TINAGL1 also activated Smad3 and increased VEGF secretion, while inhibition of Smad3 downregulated VEGF. Inhibition of this axis by blocking Smad3 or VEGF impeded the effects of TINAGL1 on HCC cell growth, proliferation, migration, and invasion. Taken together, TINAGL1 promoted HCC cell growth and proliferation by increasing VEGF production via the TGF-β/Smad3 pathway.

To summarize, TINAGL1 promoted HCC cell growth and proliferation and inhibited cell apoptosis both in vitro and in vivo, indicating its potential as a novel biomarker of HCC. Our study is the first to demonstrate that TINAGL1 drives hepatocellular carcinogenesis by activating the TGF-β signaling pathway and presents TINAGL1 as a potential new prognostic biomarker and therapeutic target for HCC.

Conclusion

TINAGL1 is upregulated in HCC tissues and promotes hepatocellular carcinogenesis via the TGF-β/Smad3/VEGF axis, indicating its potential as a novel biomarker for HCC.

Acknowledgment

This work was supported by the National Natural Science Foundation of China (81702757).

Author contributions

LS conceived the study and designed the experiments. ZD obtained the specimens. HG and ZG provided the experimental materials. All authors contributed to data analysis, drafting and revising the article, gave final approval of the version to be published, and agree to be accountable for all aspects of the work. The authors thank Professor ZY for conducting and outstanding editorial assistance.

Disclosure

The authors report no conflicts of interest in this work.

References

1. Zhu Y, Zhao L, Shi K, Huang Z, Chen B. TRIM24 promotes hepatocellular carcinoma progression via AMPK signaling. *Exp Cell Res*. 2018;367(2):274–281.
2. Xie DY, Ren ZG, Zhou J, Fan J, Gao Q. Critical appraisal of Chinese 2017 guideline on the management of hepatocellular carcinoma. *Hepatobiliary Surg Nutr*. 2017;6(6):387–396.
3. Lee D, Lee HC, An J, et al. Comparison of surgical resection versus transarterial chemoembolization with additional radiation therapy in patients with hepatocellular carcinoma with portal vein invasion. *Clin Mol Hepatol*. 2018;24(2):144–150.
4. de Oliveira RM, Ornelas Ricart CA, Araujo Martins AM. Use of mass spectrometry to screen glycan early markers in hepatocellular carcinoma. *Front Oncol*. 2017;7:328.
5. Chowdhury SM, Lee T, Bachawal SV, et al. Longitudinal assessment of ultrasound-guided complementary microRNA therapy of hepatocellular carcinoma. *J Control Release*. 2018;281:19–28.
6. Jiang W, Li G, Li W, et al. Sodium orthovanadate overcomes sorafenib resistance of hepatocellular carcinoma cells by inhibiting Na^+/K^+-ATPase activity and hypoxia-inducible pathways. *Sci Rep*. 2018;8(1):9706.
7. Li X, Xu W, Kang W, et al. Genomic analysis of liver cancer unveils novel driver genes and distinct prognostic features. *Theranostics*. 2018;8(6):1740–1751.
8. Igarashi T, Tajiri Y, Sakurai M, et al. Tubulointerstitial nephritis antigen-like 1 is expressed in extraembryonic tissues and interacts with laminin 1 in the Reichert membrane at postimplantation in the mouse. *Biol Reprod*. 2009;81(5):948–955.
9. Tajiri Y, Igarashi T, Li D, et al. Tubulointerstitial nephritis antigen-like 1 is expressed in the uterus and binds with integrins in decidualized endometrium during postimplantation in mice. *Biol Reprod*. 2010;82(2):263–270.
10. Wex T, Lipyansky A, Brömme N, Wex H, Guan XQ, Brömme D. TINag-RP, a novel catalytically inactive cathepsin B-related protein with EGF domains, is predominantly expressed in vascular smooth muscle cells. *Biochemistry.* 2001;40:1350–1357.
11. Lennon R, Byron A, Humphries JD, et al. Global analysis reveals the complexity of the human glomerular extracellular matrix. *J Am Soc Nephrol*. 2014;25(5):939–951.
12. Mary S, Kulkarni MJ, Mehendale SS, Joshi SR, Giri AP. Tubulointerstitial nephritis antigen-like 1 protein is downregulated in the placenta of pre-eclamptic women. *Clin Proteomics*. 2017;14(1):8.
13. Takahashi A, Rahim A, Takeuchi M. Impaired female fertility in tubulointerstitial antigen-like 1-deficient mice. *J Reprod Dev*. 2016;62(1):43–49.
14. Barallobre-Barreiro J, Didangelos A, Schoendube FA, et al. Proteomics analysis of cardiac extracellular matrix remodeling in a porcine model of ischemia/reperfusion injury. *Circulation*. 2012;125(6):789–802.
15. Umeyama H, Iwadate M, Taguchi Y-H. TINAGL1 and B3GALNT1 are potential therapy target genes to suppress metastasis in non-small cell lung cancer. *BMC Genomics*. 2014;15(Suppl 9):S2.
16. Korpal M, Ell BJ, Buffa FM, et al. Direct targeting of Sec23a by miR-200s influences cancer cell secretome and promotes metastatic colonization. *Nat Med*. 2011;17(9):1101–1108.
17. Naba A, Clauser KR, Lamar JM, Carr SA, Hynes RO. Extracellular matrix signatures of human mammary carcinoma identify novel metastasis promoters. *Elife*. 2014;3:e01308.
18. Sui H, Zhao J, Zhou L, et al. Tanshinone IIA inhibits β-catenin/VEGF-mediated angiogenesis by targeting TGF-β1 in normoxic and HIF-1α in hypoxic microenvironments in human colorectal cancer. *Cancer Lett*. 2017;403:86–97.
19. Sun H, Miao C, Liu W, et al. TGF-β1/TβRII/Smad3 signaling pathway promotes VEGF expression in oral squamous cell carcinoma tumor-associated macrophages. *Biochem Biophys Res Commun*. 2018;497(2):583–590.
20. Breier G, Blum S, Peli J, et al. Transforming growth factor-beta and Ras regulate the VEGF/VEGF-receptor system during tumor angiogenesis. *Int J Cancer*. 2002;97(2):142–148.
21. Jin X, Aimaiti Y, Chen Z, Wang W, Li D. Hepatic stellate cells promote angiogenesis via the TGF-β1-Jagged1/VEGFA axis. *Exp Cell Res*. 2018;373(1-2):34–43.
22. Qin X-Y, Suzuki H, Honda M, et al. Prevention of hepatocellular carcinoma by targeting MYCN-positive liver cancer stem cells with acyclic retinoid. *Proc Natl Acad Sci U S A*. 2018;115(19):4969–4974.
23. Toyoda H, Kumada T, Tada T, et al. Impact of previously cured hepatocellular carcinoma (HCC) on new development of HCC after eradication of hepatitis C infection with non-interferon-based treatments. *Aliment Pharmacol Ther*. 2018;48(6):664–670.
24. Guo T, Wang H, Liu P, et al. SNHG6 acts as a genome-wide hypomethylation trigger via coupling of miR-1297-mediated S-adenosylmethionine-dependent positive feedback loops. *Cancer Res*. 2018;78(14):3849–3864.
25. Hou G, Chen L, Liu G, et al. Aldehyde dehydrogenase-2 (ALDH2) opposes hepatocellular carcinoma progression by regulating AMP-activated protein kinase signaling in mice. *Hepatology*. 2017;65(5):1628–1644.
26. Li D, Mukai K, Suzuki T, et al. Adrenocortical zonation factor 1 is a novel matricellular protein promoting integrin-mediated adhesion of adrenocortical and vascular smooth muscle cells. *FEBS J*. 2007;274(10):2506–2522.
27. Witte D, Otterbein H, Förster M, et al. Negative regulation of TGF-β1-induced MKK6-p38 and MEK-ERK signalling and epithelial-mesenchymal transition by Rac1b. *Sci Rep*. 2017;7(1):17313.
28. Serralheiro P, Soares A, Costa Almeida C, Verde I. TGF-β1 in vascular wall pathology: unraveling chronic venous insufficiency pathophysiology. *Int J Mol Sci*. 2017;18(12):2534.
29. Ungefroren H, Witte D, Fiedler C, et al. The role of PAR2 in TGF-β1-induced ERK activation and cell motility. *Int J Mol Sci*. 2017;18(12):2776.
30. Zhang L, Zhou D, Guan W, et al. Pyridoxine 5'-phosphate oxidase is a novel therapeutic target and regulated by the TGF-β signalling pathway in epithelial ovarian cancer. *Cell Death Dis*. 2017;8(12):3214.
31. Zhu Y, Kong F, Zhang C, et al. CD133 mediates the TGF-β1-induced activation of the PI3K/ERK/P70S6K signaling pathway in gastric cancer cells. *Oncol Lett*. 2017;14(6):7211–7216.
32. Lucarelli P, Schilling M, Kreutz C, et al. Resolving the combinatorial complexity of Smad protein complex formation and its link to gene expression. *Cell Syst*. 2018;6(1):75–89e11.

Cancer Management and Research

Dovepress

Publish your work in this journal

Cancer Management and Research is an international, peer-reviewed open access journal focusing on cancer research and the optimal use of preventative and integrated treatment interventions to achieve improved outcomes, enhanced survival and quality of life for the cancer patient. The manuscript management system is completely online and includes a very quick and fair peer-review system, which is all easy to use. Visit http://www.dovepress.com/testimonials.php to read real quotes from published authors.

Submit your manuscript here: https://www.dovepress.com/cancer-management-and-research-journal